

# Morphology, crystalline structure, and chemical properties of 100 MeV Ag- ion beam irradiated polyvinylidene fluoride (PVDF) thin film

DINESH SINGH RANA\*, D. K. CHATURVEDI, J. K. QUAMARA<sup>a</sup>

*Institute of Instrumentation Engineering, Kurukshetra University, Kurukshetra-136119*

*<sup>a</sup>Department of Physics, National Institute of Technology, Kurukshetra-136119*

Thin films (12  $\mu\text{m}$ ) of polyvinylidene fluoride (PVDF) were irradiated with 100 MeV Ag- ion beam at fluence  $1.875 \times 10^{11}$  ion/cm<sup>2</sup>. The changes in physical, chemical, and surface morphological properties of irradiated films have been investigated using X-ray diffraction (XRD), Fourier Transform Infrared Spectroscopy (FTIR), Field emission scanning electron microscopy (FESEM) and Energy Dispersive Analysis by X-ray (EDAX) techniques by taking unirradiated (pristine) film as reference. The diffraction pattern of PVDF films shows this polymer is in semi-crystalline form and possesses crystalline  $\alpha$ -,  $\beta$ -, and  $\gamma$ - phases. A decrease in the crystallinity and increase in crystallite size has been observed due to 100 MeV Ag- ion irradiation. Using XRD data, the degree of crystallinity, crystallite size and other structural parameters such as micro strain and dislocation density of pristine and irradiated films have been estimated. In the FTIR spectra, no appreciable change in characteristic bands has been observed after irradiation, indicating that PVDF is chemically stable. EDAX result shows that the relative chemical composition of PVDF is invariant under energetic heavy ion irradiation. FESEM analysis shows granular microstructure with increase in grain size and porosity upon ion irradiation.

(Received February 23, 2009; accepted May 25, 2009)

*Keywords:* SHI, PVDF, FTIR, XRD, FWHM, EDAX, FESEM

## 1. Introduction

Polyvinylidene fluoride is a long chain semi-crystalline high-molecular weight polymer with repeat unit (CH<sub>2</sub> - CF<sub>2</sub>), whose structure is essentially head-to-tail, i.e., CH<sub>2</sub> - CF<sub>2</sub> - (CH<sub>2</sub>-CF<sub>2</sub>)<sub>n</sub> - CH<sub>2</sub> - CF<sub>2</sub> and has acquired immense importance in scientific and technological research because of its unique mechanical, electrical, pyroelectric, ferroelectric, piezoelectric properties and exceptional biocompatibility [1]. It is also one of the rare polymer exhibit diverse crystalline forms, having at least five phases known as  $\alpha$ ,  $\beta$ ,  $\gamma$ ,  $\delta$  and  $\epsilon$  [2-4]. The alpha ( $\alpha$ ) phase assumes a distorted trans-gauche-trans-gauche' (TG<sup>+</sup>GTG<sup>+</sup>) conformation. While there is a net dipole moment perpendicular to the chain due to the polar C-F bond, the unit cell is actually non polar. The beta phase ( $\beta$ ) assumes a distorted planar zigzag, all-trans conformation, resulting in a polar unit cell. The  $\gamma$ - phase has a structure intermediate to the helical  $\alpha$ - and zigzag  $\beta$ - phase [5]. The  $\beta$ - phase and sometimes the  $\gamma$ - phase can undergo reversible changes in polarization to create high piezoelectric and pyroelectric activity which makes this suitable polymeric material to be used in IR sensors, ultrasonic transducers, electromechanical, electro acoustic transducers [6] and micro-actuators development. The exceptional biocompatibility of PVDF film is used in the development of skin transducer, implantable medical devices and micro actuators [1].

In addition, light weight and chemical resistance of PVDF polymer promote their use for development of

micro sensors and actuators for space applications. However, in space the performance of sensors and actuators may be affected due to the strong interaction of ultraviolet,  $\gamma$ -rays, X-rays, energetic ions and atomic oxygen exposure with the sensor material. The interaction of these radiations with PVDF may change its physical, chemical, optical, structural and morphological properties. The behavior of PVDF exposed to different kinds of radiation [7-15, 20] has been studied before. These studies reveal the enhancement in electrical conductivity and change in crystallinity of PVDF [11, 12]. The decrease in crystallinity has been reported under low-energy ion implantation [11, 12, and 15] whereas an increase in crystallinity has been reported under electron, X-ray and  $\gamma$ -ray irradiations [13, 16-18]. The crystallinity plays a crucial role in determining piezoelectric, mechanical, optical, electrical and even thermal properties of polymers [11].

Swift heavy ion (SHI) irradiation is a relatively new technique for modification of polymeric material properties to promote their use for the development of sensors and actuators to radiation environmental applications. In the present paper, we investigate the physical, structural, chemical, and morphological changes in PVDF films due to SHI irradiation through the XRD, FTIR, FESEM, and EDAX techniques. The transmission electron microscopy (TEM) and electron Scanning microscopy (SEM) are mainly used to examine surface structure and inside the object (<100nm). Augmenting the TEM method with high resolution FESEM provides the

opportunity to examine the overall particle shape, surface topography, and the side and termination (particle end) geometries. To the best of our knowledge, this is the first time a detailed and comprehensive FESEM morphological characterization method has been presented for supplementing TEM analyses.

## 2. Experimental details

The poly-vinylidene fluoride used in the present study was procured from DuPont in flat film forms of 12  $\mu\text{m}$  thickness. The samples of size 1 sq. cm were irradiated with 100 MeV Ag- ion at fluence  $1.875 \times 10^{11}$  ions/cm<sup>2</sup> using the PELLETRON facility at Inter University Accelerator Centre, New Delhi. The pristine and SHI exposed PVDF films were later investigated using XRD, FTIR, FESEM, and EDAX techniques.

The XRD analysis has been done using Bruker AXS D8 Advance diffractometer with operating target voltage 40 KV and current 30mA. The XRD data were collected for angular position  $2\theta$  in the interval 10 to  $50^\circ$ , in steps of  $0.05^\circ$  in 3second, using Bruker AXS D8 powder diffractometer with copper  $K\alpha$  ( $\lambda=1.5406 \text{ \AA}$ ) radiation source at the room temperature. The FTIR analysis of samples has been done using ABB Bomen spectrometer (MBIO4E) with the ATR (attenuated total reflection) in the range  $650 - 4000\text{cm}^{-1}$ . The samples were analyzed at  $8 \text{ cm}^{-1}$  resolution and 16 scans co-averaged using the Galactic spectra Calc software. Surface morphology of pristine and irradiated films has been investigated through TEM/FESEM using Quanta 200FEG instrument system having resolution of 2nm at accelerating voltage 30 KV with magnification; 1,000,000X. The chemical compositional identification is done by EDAX using EDX - INCA 350 Energy System (Energy Dispersive X-Ray System for SEM) attached to Quanta 200FEG instrument system.

## 3. Results and data analysis

### 3.1 X-ray diffraction analysis

X-ray diffraction technique has been utilized to detect changes in crystalline and amorphous regions along with the degree of crystallinity. It is used to measure crystal structure, grain size and residual stress of materials through interaction of X-ray beams with samples. As X-rays are predominantly diffracted by electron density, analysis of the diffraction angles can be used to produce an electron density map of a given crystal or crystalline structure. The polycrystallinity of the pristine and the irradiated PVDF films are investigated using X-ray diffraction analysis.

The X-ray diffraction spectra of pristine and Ag-ion irradiated PVDF films have been illustrated in figures 1a and 1b respectively. The diffraction patterns of pristine PVDF show its semi crystalline nature. The peak positions show crystalline  $\alpha$ -,  $\beta$ -, and  $\gamma$ - phases and a broad

background due to the scattering from amorphous regions of the polymer. The XRD data, i.e. angular positions ( $2\theta$ ), peak intensity (I) and lattice spacing (d), corresponding to  $\alpha$ -,  $\beta$ -, and  $\gamma$ - phases, of pristine and Ag-ion irradiated films are summarized in table1. In conformity with other workers [7, 11, 12, 15, 19-21] the X-ray diffraction data of pristine film (figures1, table1) show characteristic strong  $\beta$ -phase peak at  $2\theta \approx 20.63^\circ$ , which is a reflection of (200) and (110) planes, characteristic strong  $\alpha$ -phase peak at  $2\theta \approx 17.77^\circ$  from the reflection of (100) plane and very weak broader peak at  $2\theta \approx 36.06^\circ$  from the reflection plane (200) is correspond to the  $\gamma$ - phase. These observations (figures1a, table1) clearly indicate that PVDF thin films possess crystalline  $\alpha$ -,  $\beta$ - and  $\gamma$ -phases.

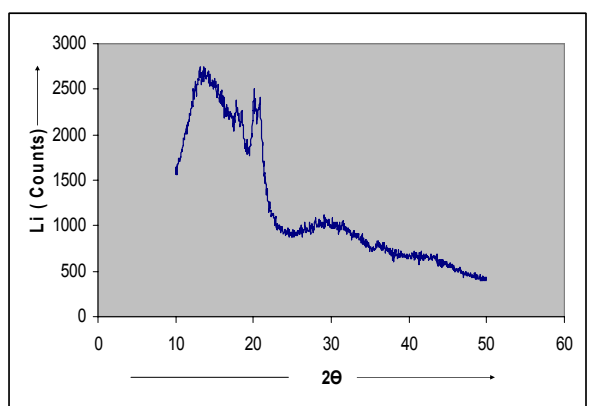
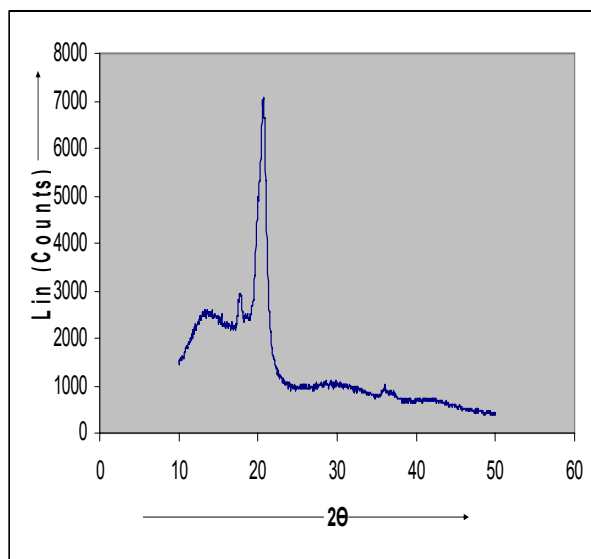


Fig. 1. XRD spectra of PVDF (a) Pristine (b) Ag-ion irradiated

In ion irradiated PVDF (Fig. 1b), the diffraction peaks corresponding to the crystalline  $\alpha$ - and  $\beta$ - phases get converted into the two closely spaced peaks at  $2\theta \approx 17.85^\circ$  -  $18.48^\circ$  with equal full width at half maxima (FWHM) and

peaks at  $2\theta \approx 20.10^\circ$ ,  $20.81^\circ$  with equal FWHM (table1) respectively. Two smaller peaks at angular position  $2\theta \approx 28.00^\circ$  with inter-planar spacing (d)  $3.184 \text{ \AA}$  and at angular position  $2\theta \approx 38.29^\circ$  with inter-planar spacing (d)  $2.348 \text{ \AA}$  are also observed in the XRD spectra of irradiated film, which can be assigned to crystalline  $\alpha$  (111) and  $\gamma$  (211) phases respectively. As compared to pristine film, the diffraction pattern of irradiated film not only shows a decrease in intensity but also shows the presence of kinks at crystalline  $\alpha$ -,  $\beta$ - and  $\gamma$ - phases peaks. The decrease in peak intensity of diffraction peaks is usually related to the decrease in crystallinity [11, 12, and 15] and the occurrence of kinks can be associated with the increase in the mean crystallite size. The decrease in crystallinity on irradiation could be due to scission processes in the main chains of PVDF leading to the disruption in packing. The increase in mean crystallite size is due to the formation of some large size crystallites in the amorphous regions of films upon irradiation. The addition of these large size crystallites with the original crystallites causes the mean size of the crystallite to increase. From the table1, we further observe that on irradiation the angular positions of  $\alpha$ - and  $\gamma$ - phases get shifted towards higher angles due to the decrease in lattice spacing (d) while the angular positions of  $\beta$ -phase get shifted towards higher and lower angles.

### 3.1.1 Crystallinity, crystallite size and other structural parameters

The degree (percentage) of crystallinity (K), mean crystallite size (D), micro strain ( $\epsilon$ ) and dislocation density ( $\delta$ ) have been estimated from the XRD pattern of pristine and swift heavy ion irradiated samples. In order to determine the crystallinity of pristine and ion irradiated samples we obtained X-ray diffractogram from their respective XRD spectra and shown in figures 2a and 2b respectively. The X-ray diffractogram for pristine PVDF has two crystalline peaks with area A1, A2, superimposed on abroad amorphous hump of left over area A5 as shown in figure 2a. The percentage of crystallinity ( $Kp$ ) can be calculated using following equation;

$$Kp = \frac{Kc(A1 + A2)}{Kc(A1 + A2) + Ka(A5)} \times 100$$

$$= \frac{(A1 + A2)}{(A1 + A2) + \frac{Ka}{Kc}(A5)} \times 100$$
(1)

Here  $Ka$  and  $Kc$  are proportionality constant for amorphous and crystalline phases respectively. This polymer is known to have nearly 50% crystalline and 50% amorphous in pristine form and hence  $Ka$  is equal to  $Kc$ . The equation (1) becomes

$$Kp = \left( \frac{\Omega_{cp}}{\Omega_{tp}} \right) \times 100$$
(2)

Here  $\Omega_{cp}$  denotes the total crystalline area and  $\Omega_{tp}$  denotes the total area under the diffractogram. The area  $\Omega_{cp}$  and  $\Omega_{tp}$  have been calculated by dividing the X-ray diffractogram into small square grids ( $0.5 \times 0.5 \text{ mm}^2$ ) and counting the number of grids.

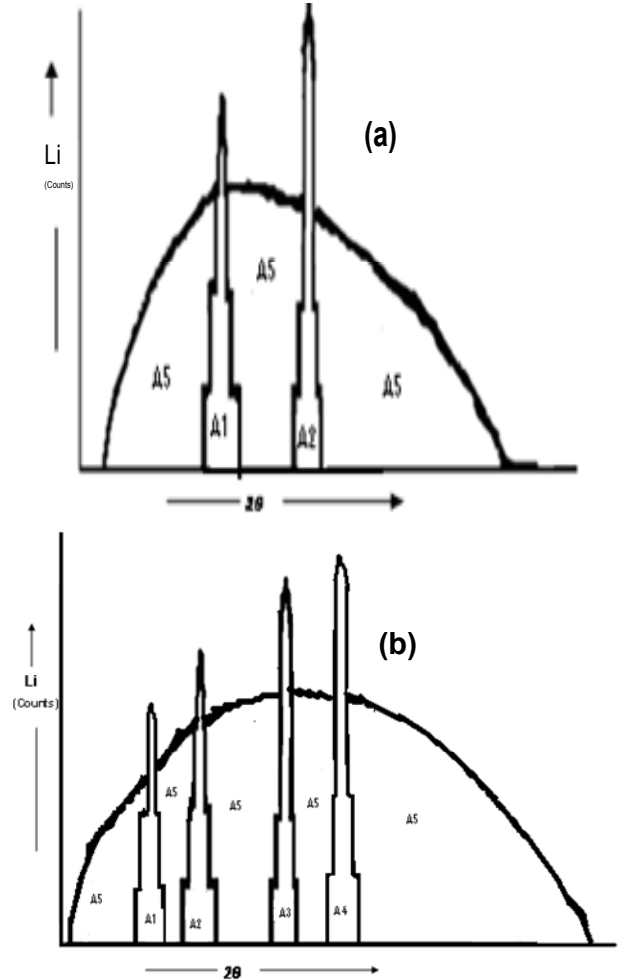


Fig. 2. XRD diffractograms for (a) Pristine, (b) Ion irradiated

For the irradiated film the X-ray diffractogram has Four crystalline peaks with area A1, A2, A3 and A4 superimposed on abroad amorphous hump of left over area A5 as shown in figure2b, then the percentage of crystallinity( $Ki$ ) can be calculated using following equation;

$$Ki = \frac{Kc(A1 + A2 + A3 + A4)}{Kc(A1 + A2 + A3 + A4) + Ka(A5)} \times 100$$

$$= \frac{(A1 + A2 + A3 + A4)}{(A1 + A2 + A3 + A4) + \frac{Ka}{Kc}(A5)} \times 100$$
(3)

Here  $K_a$  and  $K_c$  are proportionality constant for amorphous and crystalline phases respectively. For  $K_a$  equal to  $K_c$  the equation (1) becomes

$$K_i = \left( \frac{\Omega_{ci}}{\Omega_{ti}} \right) \times 100 \quad (4)$$

Here  $\Omega_{ci}$  denotes the total crystalline area and  $\Omega_{ti}$  denotes the total area under the diffractogram. The degree (percentage) of crystallinity for pristine and irradiated films is found to be approximately 52.56% and 50.28% respectively.

We estimate the crystallite size ( $D$ ) from the diffraction ray line broadening using Scherrer equation [19]:

$$D = \frac{C\lambda}{W \cos \theta} \quad (5)$$

here,  $C$  is a constant which depends on diffractometer setup,  $\lambda$  is wavelength of X-ray,  $\theta$  is diffraction angle or

Bragg's angle and  $W$  denotes FWHM. In the present setup  $C=0.9$  and  $\lambda=1.5406 \text{ \AA}$ . The values of  $W$  and  $\theta$  can be obtained from the diffraction pattern (figures 1a and b).

The micro strain ( $\epsilon$ ) and dislocation density ( $\delta$ ) have been calculated using the following relations:

$$\epsilon = \frac{1}{4} W \cos \theta \quad (6)$$

and

$$\delta = \frac{1}{D^2} \quad (7)$$

The estimated structural parameters for pristine and irradiated PVDF films have been given in table 2. We observe a significance enhancement in crystallite size in irradiated PVDF samples. This is in conformity with our interpretation of XRD spectra as discuss earlier. However we observe a decrease in micro strain ( $\epsilon$ ) and dislocation density ( $\delta$ ) in irradiation PVDF film.

Table 1. XRD Data of pristine and irradiated PVDF film

Phase	Pristine film			Irradiated Film		
	2 $\theta$	I	d( $\text{\AA}$ )	2 $\theta$	I	d( $\text{\AA}$ )
$\alpha$	17.77	2912	4.987	17.85	2385	4.963
				18.48	2243	4.796
$\beta$	20.63	6973	4.301	20.10	2511	4.422
				20.82	2354	4.263
$\gamma$	36.06	1005	2.488	38.29	702	2.348

Table 2. Structural parameter of pristine and irradiated PVDF film.

Sample	Phase	2 $\theta$ (deg)	$\theta$	cos $\theta$	W (deg)	W ( $10^{-3}$ rad)	W cos $\theta$ ( $10^{-3}$ )	D (nm)	$\epsilon$ ( $10^{-3}$ )	$\delta$ ( $10^{15}$ )
Pristine	$\alpha$	17.77	8.880	0.9980	0.50	8.722	8.617	16.08	2.154	3.8667
	$\beta$	20.63	10.315	0.9838	1.10	19.190	18.879	7.43	4.719	8.1100
Ag-ion Irradiated	$\alpha_1$	17.85	8.925	0.9878	0.25	4.363	4.311	32.15	1.077	0.9700
	$\alpha_2$	18.48	9.240	0.9870	0.20	3.490	3.444	40.24	0.861	0.6170
	$\beta_1$	20.10	10.050	0.9846	0.35	6.108	6.014	23.05	1.500	1.8820
	$\beta_2$	20.82	10.410	0.9835	0.55	9.599	9.440	14.68	2.360	4.6400

### 3.2 FTIR analysis

The FTIR spectroscopy detects the transition between energy levels in molecules which results from vibrations of inter atomic bonds and hence provides precise information about orientations of specific functional groups within the polymer. In infrared spectroscopy, the

frequency region  $650\text{-}4000 \text{ cm}^{-1}$  covers the absorption due to the fundamental vibration of almost all the common functional groups of organic compounds. The functional groups in polymers have absorption which are characteristic not only in position but also in intensity.



### 3.3 Energy dispersive analysis by X-ray (EDAX)

The EDAX microscopy is an indispensable tool for identification and measuring element composition on the surface of thin film samples of interest. The peak intensity in the Energy dispersive x-ray (EDX) spectra represents a semi-quantitative relationship of the chemical elements present in the sample. EDAX microscopy cannot identify the chemical elements having atomic weight less than four and hence we can not find hydrogen in the EDX spectra. The EDX spectra of pristine and Ag-ion irradiated 12  $\mu\text{m}$

PVDF films are illustrated in figure 5a and figure 5b respectively. Both spectra show only two peaks corresponding to main chemical elements carbon and fluorine originating from PVDF structure. We do not find any new peak in the EDX spectra of irradiated samples, which indicate that there is no formation of any new intermediate chemically distinct compound on irradiation which collaborate our FTIR findings. The appearance of third small peak in all EDX spectra represents the presence of gold electrode deposited on the films for EDAX.

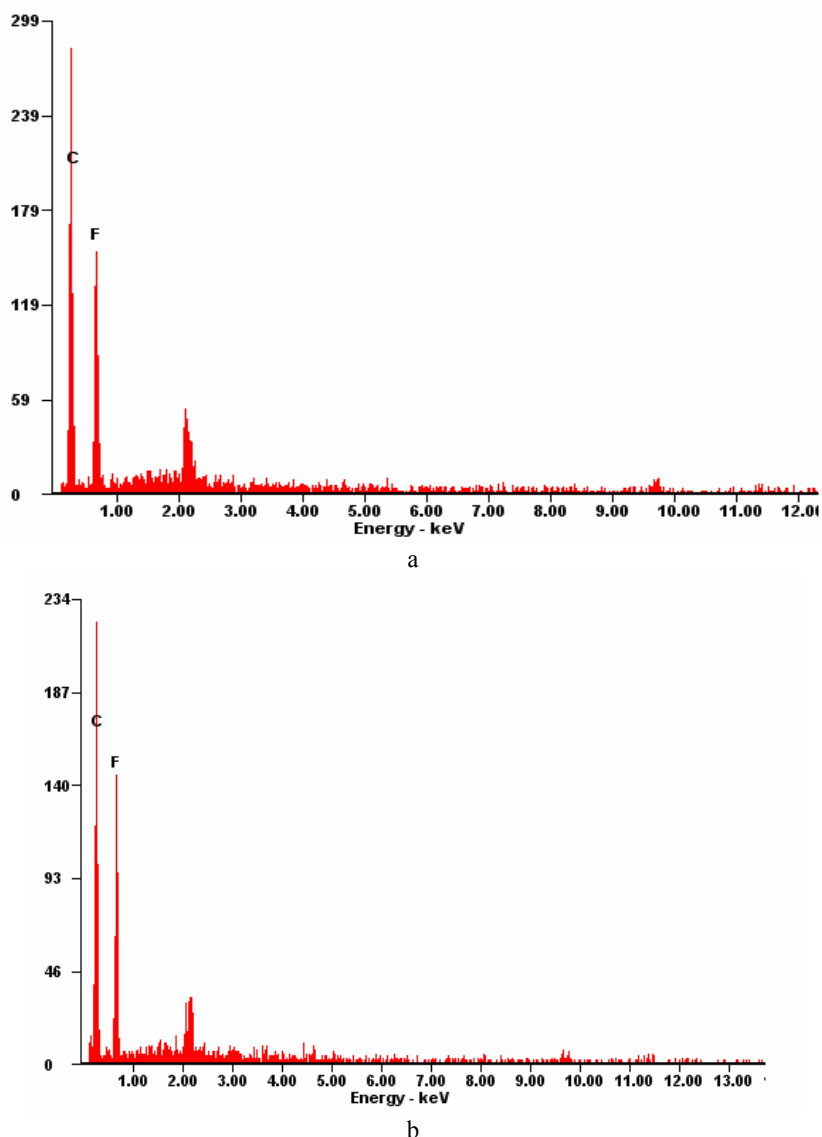


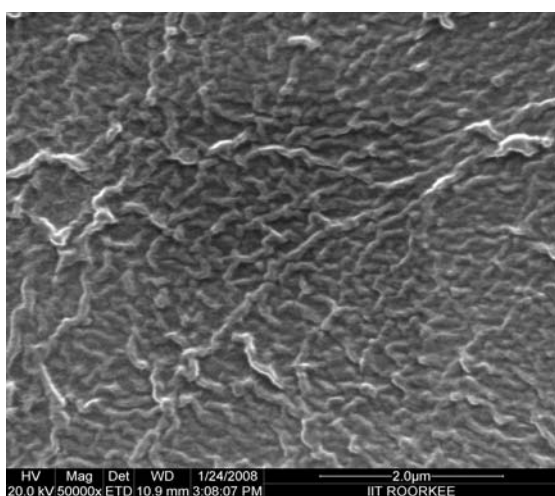
Fig. 5. EDX spectra of 12  $\mu\text{m}$  PVDF films (a) Pristine (b) irradiated

### 3.4 Field emission scanning electron microscopy (FESEM)

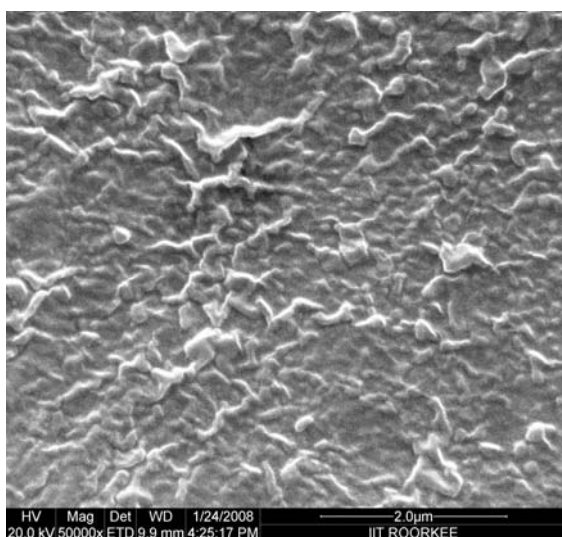
The FESEM is used for the investigation of topographic details on the surface and entire structure of

the thin films. The field emission scanning electron microscopic (FESEM) micrographs (at magnification of 50000) of pristine and 100MeV Ag-ion irradiated PVDF films are shown in figure 6a and figure 6b respectively.

Fig. 6a shows that pristine PVDF film possesses long finger/fibers chain like structures on entire surface area with small protuberance at some places and show grains of different size and nano-porous regions in between. These fibers like structures probably may be correlated to random orientation of the  $\beta$  and  $\alpha$  crystallites. On irradiation with swift heavy Ag-ion the surface morphological features such as distributions of grain shapes, size and porosity of the film changes and show increase in grain size and non uniform distribution of grains in the granular surface microstructure of the film. This change in grain shape and size is in line with our interpretation of XRD spectra and estimated crystallite size (table 2). Further, we also observe that the nanoporosity increases upon ion irradiation (figure 6b).



a



b

Fig. 6. FESEM Micrographs of 12  $\mu\text{m}$  PVDF films (a) Pristine, (b) Ag-ion irradiated.

#### 4. Conclusions

We have investigated SHI irradiation induced changes in PVDF thin film using XRD, FTIR EDAX and FESEM techniques. The XRD spectra are used to estimate structural parameters such as degree of crystallinity, crystallite size, micro strain and dislocation density of pristine and irradiated samples. The XRD analysis shows that the size of crystallites is increased while the lattice spacing and the degree of crystallinity is decreased upon irradiation. The micro strain and dislocation density also decreases upon ion irradiation. The FTIR spectra of irradiated film do not show any prominent new bands, which indicates that there is no significant formation of intermediate chemically distinct material on irradiation. EDAX results show that the relative chemical composition of PVDF remains invariant under ion irradiation. FESEM micrographs show granular and porous surface morphology with adhesivity and increased grain size and porosity upon ion irradiation.

#### Acknowledgement

Authors are grateful to the Inter University Accelerator Centre, New Delhi, for providing the irradiation facilities to carry out the research work and to Institute of Instrumentation Centre, Indian Institute of Technology, Roorkee, for extending XRD and SEM facilities.

#### References

- [1] J. Ryu et al, biosensors and bioelectronics **21**, 822 (2005)
- [2] Q. Gao, Scheinbein JI et al, Macromolecules **3**, 7564. (2000).
- [3] M. Benz, W. B. Euler et al J Appl Polym Sci **89**, 1093 (2003).
- [4] N. J. Ramer, T. Marrone, K.Stiso et al., Polymer **47**, 7160 (2006).
- [5] A. Nandi, L. Mandelkern, J. Polym. Sci. Part B: Polym. Phys. **29**, 1287. (1991).
- [6] M. A. Doverspike, M. S. Conradi, J. Appl. Phys. **2**, 65 (1989).
- [7] J. Ryu et al, biosensors and bioelectronics **21**, 822 (2005)
- [8] E. Adem, J. Rickards, G. Burillo, M. Avalos-Borja, Radiat. Phys.Chem. **54**, 637 (1999).
- [9] Z. Zhudi et. al., Radiat. Phys. Chem. **41**, 467 (1993).
- [10] N. Betz, A. Le Mole, E. Balanzat, E. Ramillon, J M Lamotte et al.; J. Polym. Sci. **B32**, 1493 (1994)
- [11] Y. Komaki, N. Ishikawa, N. Morishita etal., Radiations Measurements **26**, 123 (1996).
- [12] L. Calcagno, P. Musumeci, R. Percolla, G. Foti, Nuclear Instr. And method In Phys. Res. **B91**, 461 (1994).
- [13] A. Le Mole etal., Nucl. Instrum. & Meth. Phys. Res., **B32**, 115 (1989).
- [14] A. Lovinger J Bull. Am. Phys. Soc. **29**, 325 (1984).

- [15] Z. X. Zhen, *Radiat. Phys. Chem.* **35**, 194 (1990).
- [16] M. A. Said, C. M. Balik, *J. Polym. Sci.*, **B26**, 1457 (1988).
- [17] Y. Rosenberg, A. Sregmann, M. Narkis, S. Shkolnik, *J. Appl. Polym. Sci.* **45**, 783 (1992).
- [18] Y. Kanwano, S. Soares, *Polym. Degrade. Stab.*, **35**, 99 (1992).
- [19] Youn Mook Lim, Youn Moo Lee et al, *J. Ind. Eng. Chem.* **12**(4), 589 (2006).
- [20] B. E. Warren, *X-ray diffraction*, Dover Publication, New York, (1990).
- [21] K. D. Pae, S. K. Bhateja, et al; *J. of Polymer Sci part B; Polymer Phys.* **25**, 717 (1987).
- [22] M. Daniel, Esterly, Brian J. Love, *Journal of Polymer Science; part B Polymer Physics*, **42**(1), 91 (2004).
- [23] I. S. Elashmawi, N. A. Elsheshtawi, H. I. Abdelkader, N. A. Hakeem, *Cryst. Res. Technol.* **42**(2), 157 (2007).
- [24] T. Bocaccio, A. Bottino, G. Capaneli, A. Piaggio, *J. Membr. Sci.*, **210**(2), 315 (2002).
- [25] G. Socrates, *Infrared Characteristics, group frequencies*, John Wiley and Sons, New York 1994.
- [26] R. Gregorio Jr. et al, *Polymeric Materials Encyclopedia* Edited by J.C Salamone, CRC Press, 8 (1996).
- [27] G. Socrates, *Infrared Characteristic group Frequency*, John Wiley and Sons, New York, 1995.
- [28] N. A. Hakeem, H. I. Abdelkader, N. A. El-Sheshtawi, I. S. Elashmawi, *J. Appl. Polym. Sci.*, **102**(3), 2125 (2006).
- [29] Maneesha Garg & J K Quamara, *Indian Journal of Pure & Applied Physics* **45**, 563 (2007).

---

\*Corresponding author: dineshrana24@rediffmail.com ,  
dineshrana@yahoo.com